Cooperative defect-deformational nucleation of ordered adatom nanostructures with the participation of surface quasi-Rayleigh waves

V. I. Emel'yanov* and A. I. Mikaberidze
Physics Faculty, Lomonosov Moscow State University, 119899, Moscow, Russia
(Received 11 July 2005; revised manuscript received 24 October 2005; published 7 December 2005)

Defect-deformational mean-field theory of cooperative nucleation of ordered ensembles of nanoparticles on the isotropic surface of solids with the participation of quasistatic Rayleigh waves is developed. The system of nonlinear kinetic equations for the Fourier-amplitudes of the concentration of surface defects (adatoms or dimers) is derived and nonlinear multimode dynamics of self-organization of hexagonal ensembles of nanoparticles is described within a mean-field approximation. The mechanism of the control of the ensemble symmetry with the help of external stress is considered. The theoretical results correspond to the experimental ones obtained in studies of formation of quasihexagonal ensembles of nanoparticles under laser-controlled deposition of Ga atoms on the tip of a silica fiber.

DOI: 10.1103/PhysRevB.72.235407 PACS number(s): 68.43.Hn, 68.55.Ac, 81.16.Rf, 61.80.Ba

I. INTRODUCTION

In recent years, the spontaneous formation of periodic adatom nanostructures on the surface of solids has become the subject of intensive studies. The period, symmetric properties, and morphology of such structures are usually determined from the calculation of steady state (equilibrium) free energy of the structure.[1]

It is of great interest to study the dynamics of formation of ordered ensembles of nanoparticles on isotropic and crystalline surfaces. This would enable one to establish how the self-organization of coherent ensembles with certain symmetry occurs in dependence on the symmetry of the surface. Besides, such a study is of applied interest since it permits one to reveal mechanisms of stress-mediated control of the self-organization dynamics with the aim of directional change of resulting symmetry of the ensemble.

This work is dedicated to the description of the nonlinear multimode dynamics of formation of hexagonal ensembles of nanoparticles on the isotropic surface of solids. The consideration is carried out on the base of the mechanism of the surface defect-deformational (DD) instability in the system of mobile surface defects (adatoms or surface dimers), interacting with quasistatic surface acoustic (Rayleigh) waves.[2] The mechanism of the surface DD instability consists of the following. An initial surface fluctuation strain gives rise to strain-induced surface defect fluxes. This leads to the formation of spatially nonuniform field of surface defect concentration, which via the defect deformation potential and also via the local renormalization of the surface energy nonuniformly deforms the surface and underlying elastic continuum, increasing thus the initial strain. Exceeding a certain critical value of surface defect concentration such positive feedback leads to the onset of the DD instability with arising of nanometer scale surface relief modulations and piling up of defects at extrema of this modulation, which serve as periodic nucleation sites for the subsequent growth of nanoclusters. Each modulation (the DD grating) is characterized by a wave vector $\mathbf{q}$.

In this work the system of nonlinear kinetic equations for the Fourier-amplitudes of the concentration of the surface defects is derived in which the spatial average of the concentration of surface defects N_{d0} plays the role of the control parameter. This approach is similar to the mean-field description of critical fluctuations in the ordered phase of systems undergoing phase transitions of the second kind.[3]

The quasinonlinear analysis of this system shows that the process of formation of ordered ensemble of nanoparticles consists of four stages. At the first (linear) stage, under exceeding by the control parameter N_{d0} of the first critical value (N_{dc1}), the growth rate of DD gratings $\lambda(\mathbf{q})$ becomes positive in a certain region of values of the wave number q (the amplification band) with the center at $q=q_m$, where q_m is the wave number, at which the maximum of the growth rate is achieved. At the second stage, due to nonlinear (three-grating) interactions, triads of DD gratings are formed, in which the wave vectors $\mathbf{q}$ with the absolute values $q \approx q_m$ form equilateral triangles. To each triad a hexagonal DD structure corresponds with a random orientation on the surface. At the third stage, under exceeding of the second critical concentration of defects N_{dc2}, orientational ordering of triads occurs at a characteristic time t_θ due to interactions between them (the collapse of the angular spectrum of the DD modes in $\mathbf{q}$-space). As a result, three continua of DD gratings with wave vectors $\mathbf{q}$ lying at the angles of 60° to each other are formed. The magnitudes of the wave vectors in these continua lie inside the amplification band with the center at q_m. At the last (fourth) stage ($N_{d0} > N_{dc2}$) in each of these three continua the collapse of the spectrum of DD modes in scalar q-space occurs at a characteristic time t_m. The resulting two-dimensional Fourier-spectrum of the DD structure consists of a circle of radius $\propto q_m$ with six equidistant maxima that correspond to a perfect hexagonal DD structure. The consideration of self-organization of this hexagonal structure is carried out under the condition $t_\theta, t_m < \lambda^{-1}(q_m)$. In similar fashion the self-organization of DD structures on crystalline surface occurs, but the orientation of the dominant DD gratings in this case is determined by crystallographic directions on the surface.

The analysis of the obtained nonlinear system of kinetic equations for the Fourier amplitudes reveals also the mecha-

nism of control of the symmetry of resulting nanostructures with the help of externally applied stress. The approximate solution of the system of kinetic equations demonstrates how the stress-induced uniaxial strain of different signs amplifies or suppresses the collinear DD grating via changing anisotropically the defect diffusion coefficient.

The obtained theoretical results are compared with the results of recent experiments on formation of quasihexagonal ensembles of nanoparticles under laser-controlled deposition of Ga atoms on the tip of a silica fiber[4,5] and other experiments on self-organization of hexagonal ensembles of inhomogeneities.

We note that another important mechanism of formation of ordered surface nanostructures is the Asaro-Tiller-Grinfeld (ATG) instability.[6–9] In it the surface nanorelief formation occurs due to the competition between elastic strain energy and surface energy of the externally stressed solid surface. Similarly to the considered here DD instability, in the ATG instability the surface diffusion plays the key role in the pattern formation process. However, in the DD instability surface defects are necessary for the onset of the instability, while in ATG instability surface defects do not play any role. Besides, the DD self-organization, in contrast to the ATG instability, occurs without external stress; only the internal (self-consistent) stress induced by surface defects is involved.

II. THE SYSTEM OF KINETIC EQUATIONS FOR FOURIER AMPLITUDES OF SURFACE DEFECT CONCENTRATION

A. The equation for the concentration of surface defects

Let us consider the surface $z=0$ of a solid (z axis is directed into the medium) with mobile defects. The surface stress $\sigma_{xx}+\sigma_{yy}+\sigma_{zz}\equiv\sigma_s(x,y)$ consists of the part $\sigma_0(x,y)$ characteristic of a surface without defects and the defect-induced part $\sigma_d(x,y)$. With taking into account of the nonlocal atom-atom and defect-atom interactions, it can be written in the form of nonlocal Hooke's law:[10]

$$\begin{aligned}\sigma_s(x,y) &= \sigma_0(x,y) + \sigma_d(x,y)\\ &\equiv \int_{-\infty}^{\infty}\int_{-\infty}^{\infty}\Bigg[\int_{-\infty}^{\infty} A_0(|x-x'|,|y-y'|,|0-z'|)\\ &\quad\times\xi(x',y',z')dz'\\ &\quad + A_d(|x-x'|,|y-y'|)\xi(x',y')\Bigg]dx'dy', \end{aligned} \tag{1}$$

where $\xi(x,y)\equiv\xi(x,y,0)$ is the local surface strain. The equation for the rapidly decaying kernel A_0 is obtained in Ref. 11. It can be generalized also for the case of surface defect-atom interactions, which are assumed here to be of a long-range nature (for example, surface dipole-dipole interactions). For isotropic solids and also for cubic crystals (x and y axes coincide with directions of [100] type) the kernel $A_d(|\tau|,|\zeta|)$ is symmetric with respect to the interchange of the arguments $\tau=x-x'$ and $\zeta=y-y'$. Expanding in Eq. (1) the functions $\xi(x-\tau,y-\zeta,z')$ and $\xi(x-\tau,y-\zeta)$ in Taylor series we obtain:

$$\sigma_s(x,y) = K\xi(x,y) + Kl_d^2\Delta\xi(x,y), \tag{2}$$

where

$$\Delta = \partial^2/\partial x^2 + \partial^2/\partial y^2,$$

$$K = 3K_0,$$

$$K_0 = \int_{-\infty}^{\infty}\int_{-\infty}^{\infty}\int_{-\infty}^{\infty} A_0(|\tau|,|\zeta|,|z'|)d\tau d\zeta dz'/3$$

is the elastic modulus, determined by short-range atom-atom interactions, $l_d^2=\int_{-\infty}^{\infty}\int_{-\infty}^{\infty}A_d(|\tau|,|\zeta|)\tau^2 d\tau d\zeta/2K$, and l_d is the characteristic length of defect-atom interaction.

The work of formation of a single defect (the energy of the defect in the strain field), is written with allowance for Eq. (2) in the form

$$W_d = -\Omega_d\sigma_s = -\theta_d(\xi(x,y) + l_d^2\Delta\xi(x,y)), \tag{3}$$

where Ω_d is the change of the volume of the medium under formation of a single defect, and $\theta_d=\Omega_d K_d$ is deformation potential of the defect. The force, acting on the defect, $\mathbf{F}(\mathbf{r})=-\nabla W_d(\mathbf{r})=\theta_d\nabla(\xi+l_d^2\Delta_\parallel\xi)$, where $\mathbf{r}=(x,y)$, and $\nabla\equiv\mathrm{grad}=(\partial/\partial x,\partial/\partial y)$. The defect flux consists of diffusional and strain-induced parts:

$$\mathbf{j}_d = -D_d\nabla N_d + \frac{D_d}{k_BT}\theta_d N_d\nabla(\xi + l_d^2\Delta_\parallel\xi), \tag{4}$$

where D_d is the coefficient of surface diffusion, and k_B is Boltzman constant.

The diffusivity with allowance for strain-induced renormalization of the activation energy has the form:[12]

$$D_d = D_0\exp\left(-\frac{E_d-\theta_a\xi}{k_BT}\right) \approx D_{d0}\left(1+\frac{\theta_a\xi}{k_BT}\right), \tag{5}$$

where D_0 is a constant, E_d is the initial value of activation energy, and θ_a is the deformation activation potential of diffusion.

From the continuity equation, with allowance for defect generation and recombination, taking into account Eqs. (4) and (5), neglecting small terms formed by the multiplication of the small parameter $\theta_a\xi/k_BT$ by the dispersion term proportional to l_d^2, we obtain the nonlinear diffusion equation for the concentration of surface defects N_d (cm^{-2}):

$$\begin{aligned}\frac{\partial N_d}{\partial t} &= G_d - \frac{1}{\tau}N_d + D_{d0}\left(1+\frac{\theta_a\xi}{k_BT}\right)\Delta_\parallel N_d\\ &\quad - \frac{D_{d0}\theta_d}{k_BT}\left(1+\frac{\theta_a\xi}{k_BT}\right)N_d\Delta_\parallel\xi - \frac{D_{d0}\theta_d}{k_BT}l_d^2N_d\Delta^2\xi\\ &\quad - D_{d0}\frac{\theta_d-\theta_a}{k_BT}\nabla N_d\cdot\nabla\xi - \frac{D_{d0}\theta_d l_d^2}{k_BT}\nabla N_d\cdot\nabla(\Delta_\parallel\xi)\\ &\quad - \frac{D_{d0}\theta_d\theta_a}{(k_BT)^2}\xi\nabla N_d\cdot\nabla\xi - \frac{D_{d0}\theta_d\theta_a}{(k_BT)^2}(\nabla\xi)^2. \end{aligned} \tag{6}$$

The first term in the right-hand side of Eq. (6) takes into

account generation of mobile surface defects and the second term describes the rate of their disappearance. In the case of adatoms the first process is related to incoming of atoms at the surface and the second one to adatom desorption. In the case of formation of surface dimers (see Sec. V), G_d is the rate of dimer formation and N_d/τ is the rate of their decay. In both cases it is assumed that the generation rate G_d is spatially uniform. The nonlinear diffusion equation of different form coupled with the stress is used also in the theory of the ATG instability.[6–9]

To close Eq. (6) we need to express the strain ξ through the concentration of surface defects N_d.

B. The coupling of Fourier amplitudes of surface strain and surface defect concentration

We use for this aim the equation for the displacement vector $\mathbf{u}$ of an isotropic medium:[13,14]

$$\partial^2\mathbf{u}/\partial t^2 = c_t^2\Delta\mathbf{u} + (c_l^2 - c_t^2)\mathrm{grad}(\mathrm{div}\,\mathbf{u}), \tag{7}$$

where c_l and c_t are longitudinal and transverse sound velocities, respectively.

In the considered case of the solid half-space $z \geqslant 0$ there are two types of linearly independent solutions of Eq. (7). Besides the Rayleigh surface acoustic wave (SAW),[13,14] there is the Love wave, which exists if there is a surface layer with elastic characteristics different from those of the bulk.[14] Since this wave is transversal (the displacement vector is orthogonal to propagation direction), the surface strain $\mathrm{div}\,\mathbf{u}=0$. Thus the Love wave cannot couple with adatoms and support DD gratings. So, taking the Rayleigh SAW as a solution of Eq. (7) and generalizing it to the problem of the DD instability, we seek the solution of Eq. (7) in the form of superposition of the exponentially growing static (with the frequency $\omega=0$) quasi-Rayleigh SAW:

$$u_x = -\sum_{\mathbf{q}} iq_x R_{\mathbf{q}} \exp(i\mathbf{qr} + \lambda t - k_l z) - \sum_{\mathbf{q}} i\frac{q_x}{q} k_t Q_{\mathbf{q}} \exp(i\mathbf{qr} + \lambda t - k_t z), \tag{8}$$

$$u_y = -\sum_{\mathbf{q}} iq_y R_{\mathbf{q}} \exp(i\mathbf{qr} + \lambda t - k_l z) - \sum_{\mathbf{q}} i\frac{q_y}{q} k_t Q_{\mathbf{q}} \exp(i\mathbf{qr} + \lambda t - k_t z), \tag{9}$$

$$u_z = \sum_{\mathbf{q}} k_l R_{\mathbf{q}} \exp(i\mathbf{qr} + \lambda t - k_l z) + \sum_{\mathbf{q}} qQ_{\mathbf{q}} \exp(i\mathbf{qr} + \lambda t - k_t z), \tag{10}$$

where λ is the growth rate, R_q and Q_q are Fourier-amplitudes of fluctuation SAW, $\mathrm{q}=(q_x, q_y)$, and $k_{l,t}^2 = q^2 + \lambda^2/c_{l,t}^2$.

The surface strain ξ is expressed through the components of the displacement vector by the relation following from Eqs. (8)–(10):

$$\xi(\mathbf{r},t) = (\mathrm{div}\,\mathbf{u})_{z=0} = \sum_{\mathbf{q}} \xi_{\mathbf{q}} \exp(i\mathbf{qr} + \lambda t) = -\sum_{\mathbf{q}} \frac{\lambda^2}{c_l^2} R_{\mathbf{q}} \exp(i\mathbf{qr} + \lambda t). \tag{11}$$

The spatially nonuniform surface strain ξ causes perturbation of a uniform distribution of defects. Arising nonuniform defect concentration modulates the surface energy according to the relation $\gamma_s(\mathbf{r},t) = \gamma_{s0} + (\partial\gamma_s/\partial N_d)N_d(\mathbf{r},t)$, where the coefficient $(\partial\gamma_s/\partial N_d)$ is considered as a given parameter. This, in its turn, leads to arising of surface shear stress grad γ_s, which is compensated by the shear stress in the medium. Interaction of defects with the surface through the deformation potential θ_d leads also to arising of normal stress at the surface. Corresponding boundary conditions for the displacement vector $\mathbf{u}$ expressing the balance of shear and normal stresses at the surface, in the linear approximation by the strain, have the form

$$\left(\frac{\partial u_{x_\alpha}}{\partial z} + \frac{\partial u_z}{\partial x_\alpha}\right)_{z=0} = \left(\frac{\partial\gamma_s}{\partial N_d}\right)\frac{1}{\rho c_t^2}\frac{\partial N_d}{\partial x_\alpha},$$

$$\left[\frac{\partial u_z}{\partial z} + (1-2\beta)\left(\frac{\partial u_x}{\partial x} + \frac{\partial u_y}{\partial y}\right)\right]_{z=0} = \frac{\theta_d N_d}{\rho c_l^2 a}, \tag{12}$$

where $x_\alpha = x, y$; a is the crystal lattice parameter, ρ is the medium density, and $\beta = c_t^2/c_l^2$.

Similarly to Eq. (11), we expand the defect concentration N_d in the Fourier series:

$$N_d(\mathbf{r},t) = N_{d0} + \sum_{\mathbf{q}\neq 0} N_d(\mathbf{q})\exp(i\mathbf{q}r + \lambda t), \tag{13}$$

where N_{d0} is the spatially averaged surface defect concentration. Each pair of Fourier components $N_d(\mathbf{q})$ and $\xi(\mathbf{q})$ in Eqs. (13) and (11) describes the surface DD grating with the wave vector $\mathbf{q}$.

We add the first equality in Eq. (12), taken at $x_\alpha = x$ with the same one at $x_\alpha = y$ and substitute in the resulting equality and also in the second equality (12) the components of the displacement vector (8)–(10) and also the expansion (13). Then we obtain the system of two linear inhomogeneous equations for Fourier amplitudes of the components of the displacement vector $R_{\mathbf{q}}$ and $Q_{\mathbf{q}}$, from which we find

$$R_{\mathbf{q}} = -\frac{2k_t q^2/(k_t^2+q^2)\partial\gamma_s/\partial N_d + \theta_d/a}{\rho c_l^2[\lambda^2/c_l^2 + 2\beta q^2 - 4\beta k_l k_t q^2/(k_t^2+q^2)]} N_d(\mathbf{q}). \tag{14}$$

Using Eq. (14) in Eq. (11), we obtain the expression for the Fourier-amplitude of the strain:

$$\xi_{\mathbf{q}} = \frac{\lambda^2[2k_t q^2/(k_t^2+q^2)\partial\gamma_s/\partial N_d + \theta_d/a]}{\rho c_l^4[\lambda^2/c_l^2 + 2\beta q^2 - 4\beta k_l k_t q^2/(k_t^2+q^2)]} N_d(\mathbf{q}). \tag{15}$$

Expanding in Eq. (15) k_t and k_l in power series of the small parameter $\lambda^2/(c_{l,t}^2 q^2)$, we find the sought link between the Fourier amplitudes of the strain and surface defect concentration:

$$\xi_{\mathbf{q}} = \eta_d(q) N_d(\mathbf{q}), \tag{16}$$

where the coefficient of the DD coupling is

$$\eta_d(q) = \left[q\left(\frac{\partial \gamma_s}{\partial N_d}\right) + \frac{\theta_d}{a} \right] \Big/ [\rho c_l^2 (1-\beta)]. \tag{17}$$

C. System of kinetic equations for Fourier amplitudes of concentration of surface defects

We substitute the expansions (13) and (11) with the use of Eq. (16) in Eq. (6) and, after a transformation, obtain the system of kinetic equations for Fourier amplitudes of the concentration of surface defects in the cubic approximation:

$$\frac{\partial N_d(\mathbf{q})}{\partial t} = \lambda(q) N_d(\mathbf{q}) + \sum_{\mathbf{q}' \neq 0} K(\mathbf{q}, \mathbf{q}') N_d(\mathbf{q}') N_d(\mathbf{q} - \mathbf{q}') + \sum_{\mathbf{q}', \mathbf{q}''} K(\mathbf{q}, \mathbf{q}', \mathbf{q}'') N_d(\mathbf{q}') N_d(\mathbf{q}'') N_d(\mathbf{q} - \mathbf{q}' - \mathbf{q}''), \tag{18}$$

where the matrices of intermode interaction

$$K(\mathbf{q}, \mathbf{q}') = D_{d0} \frac{\theta_d}{k_B T} [q'^2 + \mathbf{q}(\mathbf{q} - \mathbf{q}')(1 - l_d^2 (\mathbf{q} - \mathbf{q}')^2)] \times \eta_d(q - q'), \tag{19}$$

$$K(\mathbf{q}, \mathbf{q}', \mathbf{q}'') = D_{d0} \frac{\theta_d \theta_a}{(k_B T)^2} (\mathbf{q} - \mathbf{q}' - \mathbf{q}'') \times (\mathbf{q} + \mathbf{q}' - \mathbf{q}'') \eta_d(q'') \eta_d(q - q' - q''), \tag{20}$$

the growth rate of DD gratings

$$\lambda(q) = D_{d0} q^2 \left[\frac{\theta_d N_{d0}}{(1-\beta) k_B T \rho c_l^2} (1 - l_d^2 q^2) \left(q \frac{\partial \gamma_s}{\partial N_d} + \frac{\theta_d}{a} \right) - 1 \right] - \frac{1}{\tau}, \tag{21}$$

where the uniform surface defect concentration $N_{d0} = N_d(\mathbf{q}' = 0)$ satisfies the equation:

$$\frac{\partial N_{d0}}{\partial t} = G_d - \frac{1}{\tau} N_{d0}.$$

In the following the steady state conditions are assumed and $N_{d0} = G_d \tau$ is considered as a given control parameter.

The second term in the right-hand side of Eq. (18) describes the interaction of three DD gratings, and the third term describes four-grating interactions corresponding to diffusional nonlinearity and also at $q' = -q'' = q$ the intramode (cubic) nonlinearity, which describes the stabilization of the DD instability. We study the effect of intramode nonlinearity in Sec. IV D.

Let us consider Eq. (18) first in the linear approximation.

III. THE GROWTH RATE OF SURFACE DD GRATINGS

At the linear stage, each DD grating with wave vector $\mathbf{q}$ in Eq. (13) evolves independently of the others according to the law

$$\frac{\partial N_d(\mathbf{q})}{\partial t} = \lambda(q) N_d(\mathbf{q}), \tag{22}$$

where the growth rate of the DD grating $\lambda(q)$ is defined by Eq. (21).

To elucidate the dependence (21) we assume that in the region of q values of interest the normal stress dominates ($|\theta_d|/a \gg q|\partial \gamma_s / \partial N_d|$). Then, from Eq. (21) we obtain the following expression for the growth rate:

$$\lambda(q) = D_{d0} q^2 \left[\frac{N_{d0} \theta_d^2}{(1-\beta) a \rho c_l^2 k_B T} (1 - l_d^2 q^2) - 1 \right] - \frac{1}{\tau}. \tag{23}$$

The growth rate $\lambda(q)$ reaches maximum at

$$q = q_m = \frac{1}{\sqrt{2} l_d} (1 - N_{dc1}/N_{d0})^{1/2}. \tag{24}$$

Here

$$N_{dc1} = (1-\beta) \frac{a \rho c_l^2 k_B T}{\theta_d^2} \tag{25}$$

is the critical value of the control parameter, at exceeding of which the formation of periodic structure becomes possible (at $N_{d0} > N_{dc1}$ wave number q_m becomes real). The corresponding period $\Lambda_m = 2\pi/q_m$ of the dominant grating

$$\Lambda_m = \sqrt{8} \pi l_d (1 - N_{dc1}/N_{d0})^{-1/2}. \tag{26}$$

The maximum growth rate

$$\lambda_m \equiv \lambda(q_m) = \frac{D_{d0}}{4 l_d^2} \frac{(N_{d0}/N_{dc1} - 1)^2}{N_{d0}/N_{dc1}} - \frac{1}{\tau}. \tag{27}$$

The critical value of the control parameter $\bar{N}_{dc1}$ at exceeding of which the onset of the instability occurs (at $N_{d0} > \bar{N}_{dc1}$ we have $\lambda_m > 0$) is determined from the condition $\lambda_m = 0$. In the case when adatom desorption rate or dimer decay rate are low ($\tau^{-1} \to 0$) we have $\bar{N}_{dc1} \approx N_{dc1}$. Near the threshold ($N_{d0}/\bar{N}_{dc1} \to 1$) the time of formation of the DD grating $\lambda_m^{-1} \to \infty$, that is critical slowing down takes place, which is characteristic for phase transitions.

At a constant concentration of surface defects ($N_{d0} = \text{const}$) the period depends on the temperature, at which the nucleation takes place:

$$\Lambda_m = \sqrt{8} \pi l_d (1 - T/T_c)^{-1/2}, \tag{28}$$

where the critical temperature

$$T_c = \frac{\theta_d^2 N_{d0}}{(1-\beta) a \rho c_l^2 k_B}. \tag{29}$$

According to Eq. (28), the formation of the surface DD grating is possible only at sufficiently low temperatures $T < T_c$,

and its period critically increases when the temperature $T \to T_c$.

The nanoparticle growth occurs at nucleation centers—extrema of the superpositional DD structure (see Sec. IV). The distance between the nucleation centers is determined by the period of the DD grating [Eqs. (26) and (28)]. In a virtually close-packed arrangement of nanoparticles the period of DD grating corresponds to the characteristic size of a nanoparticle in the ensemble.

Now let us consider the nonlinear stage of formation of hexagonal surface nanostructures.

IV. QUASINONLINEAR DYNAMICS OF SELF-ORGANIZATION OF HEXAGONAL DD STRUCTURES ON ISOTROPIC SURFACE

In the following, we assume, as in Eq. (23), that the normal stress dominates. Then, from Eq. (17) we obtain that the coefficient of the DD coupling in Eqs. (19) and (20) is independent of q and has the form:

$$\eta_d = \theta_d/[a(1-\beta)\rho c_l^2]. \tag{30}$$

In the following we use Eq. (30) in kinetic equations (18)–(20) for description of hierarchy of DD self-organization stages.

A. Three-grating interactions and formation of triads of DD gratings (hexagons)

As it is shown in Sec. III, at the first stage of DD self-organization the band of wave numbers q is selected with the center at $q=q_m$ and the directions of corresponding wave vectors $\mathbf{q}$ are distributed randomly on the surface.

Let us consider three DD gratings with wave vectors $\mathbf{q}_1$, $\mathbf{q}_2$, and $\mathbf{q}_3$ with the magnitudes $|\mathbf{q}_1|=|\mathbf{q}_2|=|\mathbf{q}_3|=q_m$, forming an equilateral triangle: $\mathbf{q}_1+\mathbf{q}_2+\mathbf{q}_3=0$ (the triad) with random orientation on the surface. Neglecting in Eq. (18) cubic terms (which are responsible for the saturation of unstable modes growth) and assuming that $N_{d0} \gg N_{dc1}$ and $\tau^{-1} \to 0$, we obtain the system of three equations describing this triad:

$$\frac{\partial N_d(\mathbf{q}_1)}{\partial t} = \lambda_m N_d(\mathbf{q}_1) + K N_d^*(\mathbf{q}_2) N_d^*(\mathbf{q}_3), \tag{31}$$

$$\frac{\partial N_d(\mathbf{q}_2)}{\partial t} = \lambda_m N_d(\mathbf{q}_2) + K N_d^*(\mathbf{q}_3) N_d^*(\mathbf{q}_1), \tag{32}$$

$$\frac{\partial N_d(\mathbf{q}_3)}{\partial t} = \lambda_m N_d(\mathbf{q}_3) + K N_d^*(\mathbf{q}_1) N_d^*(\mathbf{q}_2), \tag{33}$$

where λ_m is given by Eq. (27), $K=(3D_{d0}\theta_d/2k_BT)\eta_d q_m^2 > 0$. We note that, in principle, one should sum second terms in the right-hand side of Eqs. (31)–(33) over $\mathbf{q}_2$, $\mathbf{q}_3$, and $\mathbf{q}_1$, respectively, using that $\mathbf{q}_1+\mathbf{q}_2+\mathbf{q}_3=0$ and the condition that magnitudes of all wave vectors lie in the amplification band. Since Eqs. (31)–(33) illustrate here only the triad conception, we omit this summation, which can be taken into account in numerical studies.

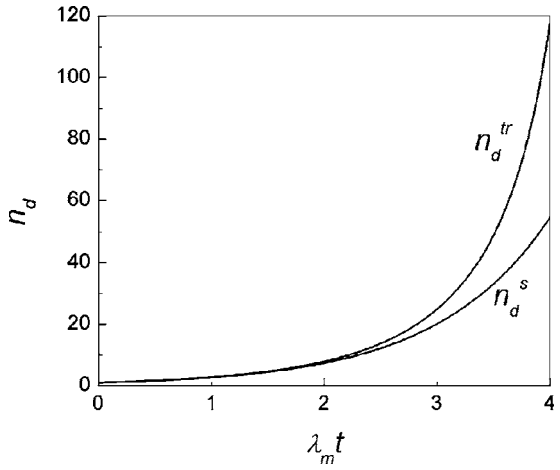

FIG. 1. Time dependence of the amplitude of a single DD grating $n_d^s=N_d^s(\lambda_m t)/N_0=\exp(\lambda_m t)$ and the amplitude of a DD grating in a triad constructed using the formula $n_d^{tr}=N_d^{tr}(\lambda_m t)/N_0=\exp(\lambda_m t)/[1+(KN_0/\lambda_m)(1-\exp(\lambda_m t))]$ [see Eq. (35)], where $KN_0/\lambda_m=3N_0/N_{d0}=10^{-2}$.

From Eqs. (31)–(33) it is seen that in the triad three DD gratings are cyclically coupled with each other. The system of equations (31)–(33) is invariant under cyclic permutation $\mathbf{q}_1 \to \mathbf{q}_2 \to \mathbf{q}_3 \to \mathbf{q}_1$. Thus, if we assume that at the initial moment $N_d(\mathbf{q}_1, t=0)=N_d(\mathbf{q}_2, t=0)=N_d(\mathbf{q}_3, t=0)\equiv N_0$, we have at all later time moments $N_d(\mathbf{q}_1, t)=N_d(\mathbf{q}_2, t)=N_d(\mathbf{q}_3, t) \equiv N_d(t)$. Then, Eq. (31) acquires the form

$$\frac{\partial N_d(t)}{\partial t} = \lambda_m N_d(t) + K N_d^2(t). \tag{34}$$

The solution of Eq. (34) with the initial condition $N_d(t) = N_0$ has the form

$$N_d(t) = \frac{N_0 \lambda_m \exp(\lambda_m t)}{\lambda_m + K N_0[1-\exp(\lambda_m t)]}. \tag{35}$$

At small values of t the amplitude of DD grating in the triad grows exponentially, $N_d(t) \approx N_0 \exp(\lambda_m t)$, in the same way as an individual grating does, but at later times the exponential growth is replaced by the explosive one for which the quadratic term in Eq. (34) is responsible. Because of that a triad grows much faster than a single DD grating (see Fig. 1).

In the following we assume that DD gratings selected at the first stage in the amplification band centered at q_m are coupled in triads (hexagons) with random orientation on the surface (the second stage of DD self-organization).

B. Collapse of angular q-spectrum of DD modes: Formation of quasihexagonal surface DD structure

Thus, after the second stage of self-organization, the DD system consists of the aggregate of triads of DD gratings randomly oriented on the surface. The wave numbers of triads lie inside the amplification band $\lambda > 0$ centered at $q=q_m$. The width of the distribution of triads over q values is much less than the width of the amplification band due to the exponential narrowing with time of the amplification band.

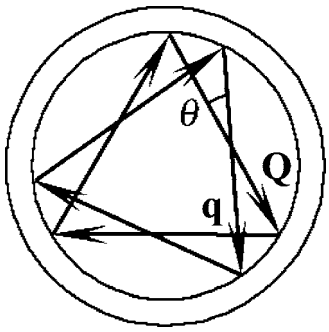

FIG. 2. The wave vector **q** of the triad under consideration is rotated by an angle θ with respect to the wave vector **Q** of the seeding triad. Magnitudes of wave vectors are distributed in the vicinity of q_m in the ring of finite thickness.

Let us assume that due to a fluctuation several triads have synchronized their orientations and formed a seeding hexagon. Let **Q** be the wave vector of one of the DD gratings of this seeding hexagon ($|\mathbf{Q}|=q_m$). Consider a triad with one of the wave vectors equal to **q** ($|\mathbf{q}|=q_m$), which form an angle θ with the vector **Q** (Fig. 2). Let us describe the temporal evolution of angular distribution of such triads assuming that the seeding hexagon does not change its orientation. We put in Eq. (18) $|\mathbf{q}-\mathbf{q}'|=|\mathbf{q}|=q_m=$const and confine the consideration to small values of q', i.e., small polar angles θ. We put also $\mathbf{q}'=-\mathbf{Q}$ and $\mathbf{q}''=\mathbf{Q}$ in the cubic term of Eq. (18). Then for the growth rate of the angular distribution of triads

$$N_d(\theta,t)=N_d(\mathbf{q},t)_{|\mathbf{q}|=q_m}$$

we obtain the following expression:

$$\lambda=\lambda_m-|\sigma_\theta|\theta^2.$$

Here the parameter of steepness of the parabolic dependence is given by

$$|\sigma_\theta|=\frac{D_{d0}}{2}\frac{|\theta_d\theta_a|}{(k_BT)^2}q_m^2\eta_d^2|N_d(\mathbf{Q})|^2, \tag{36}$$

where the Fourier amplitude of the seeding hexagon $N_d(\mathbf{Q})$ is assumed to be given. In writing down Eq. (36) and in the following it is assumed that $\theta_d\theta_a<0$ (for example, for interstitials in Si $\theta_d>0$, $\theta_a<0$).[12]

Let us expand $N_d(\mathbf{q}-\mathbf{q}')$ in Eq. (18) in power series of $\mathbf{q}'$ in polar coordinates, assuming that in the process of angular self-organization $|\mathbf{q}|=$const. Then, neglecting the angular drift, we obtain the equation of angular diffusion:

$$\frac{\partial N_d(\theta)}{\partial t}=-|D_\theta|\frac{\partial^2 N_d(\theta)}{\partial\theta^2}+(\lambda_m-|\sigma_\theta|\theta^2)N_d(\theta). \tag{37}$$

Here the modulus of negative coefficient of angular diffusion at $N_{d0}\gg N_{dc1}$ is written as

$$|D_\theta|=\frac{D_{d0}|\theta_d\eta_d|}{2k_BT}(N_{d0}/N_{dc2}-1)\sum_{\mathbf{q}'\neq 0}q'^2N_d(\mathbf{q}'), \tag{38}$$

where the coefficient of the DD coupling η_d is given by Eq. (30). In the following we assume that the long wavelength part of the DD spectrum ($|\mathbf{q}'|\ll q_m$) remains unchanged or is slow varying during the process of self-organization so that we consider the function $N_d(\mathbf{q}')$ in Eq. (38) as a given one.

In writing down Eq. (37) it is assumed that the surface defect concentration N_{d0} exceeds the second critical value

$$N_{dc2}=\frac{k_BT}{4|\theta_a\eta_d|}=(1-\beta)\frac{a\rho c_l^2k_BT}{4|\theta_d\theta_a|} \tag{39}$$

(otherwise, the angular diffusivity in Eq. (37) is positive).

We adopt the initial condition corresponding to uniform angular distribution of triads and zero boundary condition at infinity [see discussion after Eq. (47)]:

$$N_d(\theta,t=0)=N_0, \tag{40}$$

$$N_d(\theta=\pm\infty,t)=0. \tag{41}$$

We use in Eq. (37) the Fourier expansion of the function $N_d(\theta)$:

$$N_d(\theta)=\int N_d(k)\exp(i\theta k)dk, \tag{42a}$$

$$N_d(k)=\frac{1}{2\pi}\int N_d(\theta)\exp(-i\theta k)dq. \tag{42b}$$

Substituting Eq. (42a) into Eq. (37) and solving the resulting equation, we obtain:

$$N_d(k,t)=\exp\left[\left(|D_\theta|k^2+\lambda_m-|\sigma_\theta|\frac{\partial^2}{\partial(ik)^2}\right)t\right]N_d(k,t=0). \tag{43}$$

We substitute Eq. (43), where we make the substitution $t=-t'$, in Eq. (42a) and, with the use of Eq. (42b), obtain:

$$N_d(\theta,t)=\int G(\theta,\theta')N_d(\theta',0)d\theta', \tag{44}$$

where the Green function

$$\begin{aligned}G(\theta,\theta')&=\frac{1}{2\pi}\int\exp[-(|D_\theta|k^2\\&\quad+\lambda_m-|\sigma_\theta|\theta'^2)t'+i(\theta-\theta')k]dk\\&=\frac{\exp[-(\lambda_m-|\sigma_\theta|\theta'^2)t']}{(4\pi|D_\theta|t')^{1/2}}\exp\left(-\frac{(\theta-\theta')^2}{4|D_\theta|t'}\right).\end{aligned} \tag{45}$$

After integration and substituting back $t'\to -t$, we obtain the solution of Eq. (37), which is convenient to present in the form:

$$\begin{aligned}N_d(\theta,t)=N_0\exp(\lambda_m t)\left(\frac{\pi}{|\sigma_\theta|t}\right)^{1/2}\left[\left(\frac{|\sigma_\theta|t}{\pi(1-t^2/t_\theta^2)}\right)^{1/2}\right.\\\left.\times\exp\left(-\frac{\theta^2|\sigma_\theta|t}{1-t^2/t_\theta^2}\right)\right],\end{aligned} \tag{46}$$

where we introduced the time of angular collapse

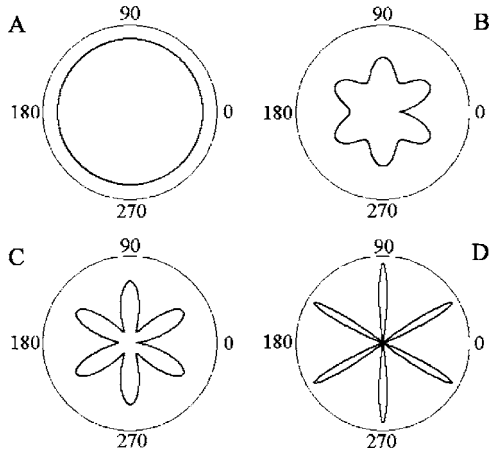

FIG. 3. The angular dependence of dimensionless Fourier-amplitude of the concentration of surface defects $N(\theta,\tau_\theta)/N(\theta,0)$ at four different time moments $\tau_\theta=t/t_\theta$ (θ is a polar angle). The dependence is given by the formula $N(\theta,\tau_\theta)/N(\theta,0)=\Sigma_{k=0}^{5}\exp(\Lambda_\theta\tau_\theta-\Delta(\theta-\pi/6-k\pi/3)^2\tau_\theta/(1-\tau_\theta^2))/(1-\tau_\theta^2)^{1/2}$, where dimensionless growth rate $\Lambda_\theta=\lambda_m t_\theta=0.03$, $\Delta=|\sigma|t_\theta=9$. (A) $\tau_\theta=0$; (B) $\tau_\theta=0.4$; (C) $\tau_\theta=0.6$; and (D) $\tau_\theta=0.95$.

$$t_\theta=\left(\frac{1}{4|D_\theta\sigma_\theta|}\right)^{1/2}. \tag{47}$$

The function in the square brackets in Eq. (46) is the Gaussian distribution with the dispersion $\langle\theta^2\rangle=(1-t^2/t_\theta^2)/(2|\sigma_\theta|t)$. This solution satisfies the initial condition (40) and the boundary conditions (41). It satisfies Eq. (37) asymptotically at $t\to t_\theta$ that can be verified by the substitution of Eq. (46) into Eq. (37) with the use of $\theta^2=(1-t^2/t_\theta^2)/(2|\sigma_\theta|t)$. We consider small values of the polar angle θ and the solution of Eq. (37) decays exponentially rapidly with increase of θ, so the use of the boundary condition (41) is justified. We note that the solution quite similar to Eq. (46) takes place when instead of uniform initial distribution (40) a broad Gaussian distribution is used, which conforms to the boundary condition (41). The numerical solution of Eq. (37) agrees well with the asymptotic solution (46).

From Eq. (46) it is seen that the ascending angular diffusion leads, with time, to the narrowing of the angular spectrum and its collapse at time moment $t=t_\theta$ into the δ function:

$$N_d(\theta,t_\theta)=N_0\exp(\lambda_m t_\theta)\left(\frac{\pi}{|\sigma_\theta|t_\theta}\right)^{1/2}\delta(\theta). \tag{48}$$

Simultaneously with narrowing of the distribution of directions of vectors **q** relative to the vector **Q** (Fig. 2) the same occurs with the distribution of directions of vectors **−q** relative to the vector **−Q** (and also with similar pairs of distributions of directions of wave vectors of triads around two other vectors of the seeding triad). As a result, with approaching the characteristic time of angular collapse t_θ the overall angular distribution narrows with the formation of six maxima along six directions (see Fig. 3). This corresponds to the angular ordering of triads, the orientation of which is foisted on by the orientation of the seeding triad (spontaneous breaking of the symmetry of triad rotation).

Thus, as a result of the third stage of self-organization—the angular ordering of triads, three continua of DD gratings are formed rotated relative to each other by the angle of 60° with the magnitudes of wave vectors **q** in each continuum lying in the vicinity of q_m inside the amplification band. In the coordinate space this corresponds to quasihexagonal periodic DD structure.

Thus after the angular DD self-organization the quasihexagonal structure is formed.

C. Collapse of the spectrum of DD modes in scalar q-space: Formation of hexagonal surface DD structure

In this section we show that due to intergrating interactions, the monochromatization of the spectrum of DD modes in the space of wave numbers q occurs independently in each of three continua, comprising the quasihexagonal DD structure.

Let us consider one such continuum with wave vectors **q** collinear to the vector **Q** of the seeding hexagon (Fig. 2). Then, in Eq. (18) we have $N_d(\mathbf{q})=N_d(q)$, $K(\mathbf{q},\mathbf{q}')=K(q,q')$, $K(\mathbf{q},\mathbf{q}',\mathbf{q}'')=K(q,q',q'')$, where q can take both positive and negative values. Putting in Eqs. (18) and (20) $q''=0$ $[N_d(q''=0)=N_{d0}]$, we reduce Eq. (18) to quadratic form

$$\frac{\partial N_d(q)}{\partial t}=\lambda(q)N_d(q)+\sum_{q_1\neq 0}\gamma(q,q')N_d(q')N_d(q-q'), \tag{49}$$

where the growth rate is given by Eq. (23) and the matrix of effective three-grating interactions, assuming that $q'\ll q$ is

$$\gamma(q,q')=K(q,q')+N_{d0}[K(q,q''=0,q')+K(q,q',q''=0)]$$
$$\approx D_{d0}\frac{|\theta_d\eta_d|}{k_BT}[q^2(1-l_d^2q^2-N_{d0}/N_{dc2})]. \tag{50}$$

Let us expand $\lambda(q)$ in Eq. (49) in Taylor series in the neighborhood of $q_m>0$:

$$\lambda(q)\approx\lambda_m-|\sigma_m|(q-q_m)^2, \tag{51}$$

where λ_m is the maximum value of the growth rate ($N_{d0}>N_{dc1}$) given by Eq. (27), $|\sigma_m|=(d^2\lambda/dq^2)_{q=q_m}=4D_{d0}(N_{d0}/N_{dc1}-1)$.

We expand $N_d(q-q')$ in Eq. (49) in power series of q' up to the terms of second order. As a result, we obtain (neglecting drift) the diffusion equation in q-space with allowance for the growth of Fourier amplitudes. In the approximation of constant coefficient of diffusion $D_q=D_m$ equal to its value at $q=q_m$, and under the condition $N_{d0}>N_{dc2}$, this equation has the form

$$\frac{\partial N_d(q)}{\partial t}=-|D_m|\frac{\partial^2N_d(q)}{\partial q^2}+[\lambda_m-|\sigma_m|(q-q_m)^2]N_d(q), \tag{52}$$

where the magnitude of the negative diffusion coefficient ($N_{d0}\gg N_{dc1}$)

$$|D_m| = D_{d0}\frac{|\theta_d \eta_d|}{2k_B T} q_m^2 (N_{d0}/N_{dc2} - 1) \sum_{q' \neq 0} q'^2 N_d(q'). \quad (53)$$

The initial condition has the form

$$N_d(q, t=0) = N_0, \quad (54a)$$

and the boundary condition:

$$N_d(q = \pm\infty) = 0. \quad (54b)$$

We expand $N_d(q)$ in Fourier integral:

$$N_d(q) = \int N_d(k)\exp(iqk)dk,$$

$$N_d(k) = \frac{1}{2\pi}\int N_d(q)\exp(-iqk)dq. \quad (55)$$

The subsequent steps of finding the solution of Eq. (52) are similar to Sec. IV C. Finally, we obtain

$$N_d(q,t) = N_0 \exp(\lambda_m t)\left(\frac{\pi}{|\sigma_m|t}\right)^{1/2}\left\{\left[\frac{|\sigma_m|t}{\pi(1 - t^2/t_m^2)}\right]^{1/2} \times \exp\left[-\frac{(q-q_m)^2|\sigma_m|t}{1 - t^2/t_m^2}\right]\right\}, \quad (56)$$

where the time of collapse in the scalar q-space is introduced:

$$t_m = \left(\frac{1}{4|D_m\sigma_m|}\right)^{1/2}. \quad (57)$$

The solution (56), satisfying Eq. (52) asymptotically at $t \to t_m$, describes the narrowing with time of DD spectrum in q space. At $t = t_m$ the spectrum collapses into the δ function:

$$N_d(q, t_m) = N_0 \exp(\lambda_m t_m)\left(\frac{\pi}{|\sigma_m|t_m}\right)^{1/2}\delta(q - q_m), \quad (58)$$

this corresponds to the generation of a single DD grating with the wave number $q = q_m$. In Fig. 4 the Fourier amplitude of the surface defect concentration, (56), is presented in dependence on the wave number q at different time moments.

Simultaneously the same behavior reveals the spectrum in the region of negative values of q, which collapses into δ function centered at $q = -q_m$. This double collapse occurs in the continuum of the wave numbers corresponding to the vectors **q** collinear to the vector **Q** in Fig. 2. With taking into account that similar double collapses occur also in two other continua of wave numbers corresponding to two other vectors of the seeding triad in Fig. 2, we obtain that as a result of the last (fourth) stage of self-organization in the two-dimensional **q** space six δ-like maxima lying equidistantly on the circle with radius $q = q_m$ are formed, that corresponds to the formation of a perfect hexagonal surface defect structure.

Thus after the fourth stage of the DD self-organization the perfect hexagonal surface defect structure is formed.

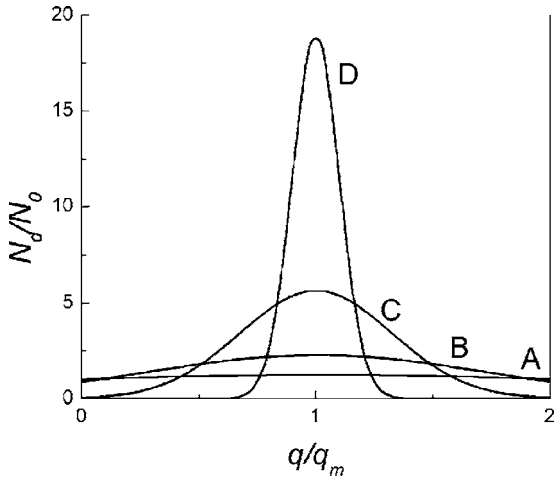

FIG. 4. The dependence of dimensionless Fourier amplitude of the concentration of surface defects on the wave number and time according to the formula $N_d(q,\tau_m)/N_0 = \exp(\Lambda_m\tau_m - [\alpha(Q-1)^2\tau_m]/(1-\tau_m^2))/(1-\tau_m^2)^{1/2}$, where $N_0 = N_d(q,0)$, where dimensionless time $\tau_m = t/t_m$, wave number $Q = q/q_m$, growth rate $\Lambda_m = \lambda_m t_m = 1$, and $\alpha = |\sigma_m| q_m^2 t_m = 1$. (A) $\tau_m = 0.2$; (B) $\tau_m = 0.6$; (C) $\tau_m = 0.9$; and (D) $\tau_m = 0.99$.

D. Stress-controlled selection of DD gratings and the change of the symmetry of the nanoparticle ensemble

In this section we show that applying the uniaxial stress enables one to effectively select DD gratings in the hexagonal structure and thus affect the symmetry of the self-organized nanoparticle ensemble in a desirable way (for example, to transform the hexagonal structure into the one-dimensional grating).

We derive from the general system of kinetic equations (18) a system of three equations for $N_d(\mathbf{q}_1)$, $N_d(\mathbf{q}_2)$, and $N_d(\mathbf{q}_3)$, describing a triad, in which wave vectors $\mathbf{q}_1$, $\mathbf{q}_2$, and $\mathbf{q}_3$ form an equilateral triangle, but here, in contrast to the system (31)–(33), we take into account also cubic terms. We retain in this system only contributions involving selectively amplified amplitudes with $|\mathbf{q}_1| = |\mathbf{q}_2| = |\mathbf{q}_3| = q_m$, neglecting all other gratings. The external compressive stress (the corresponding strain $\xi_e < 0$), which is assumed to be applied along the wave vector $\mathbf{q}_3$, in accordance with Eq. (5), increases ($\theta_a < 0$) the coefficient of diffusion along this direction. To take this into account we make the substitution $D_{d0} \to D_{d0} = D_{d0}(1 + |\theta_a \xi_e|/k_B T)$ in the equation for $N_d(\mathbf{q}_3)$. Then, the system of three equations for $N_d(\mathbf{q}_i)$ takes the following form:

$$\frac{\partial N_d(\mathbf{q}_1)}{\partial t} = \lambda_m N_d(\mathbf{q}_1) + K N_d(\mathbf{q}_2) N_d(\mathbf{q}_3) - \gamma N_d(\mathbf{q}_1)[N_d(\mathbf{q}_1)^2 + N_d(\mathbf{q}_2)^2 + N_d(\mathbf{q}_3)^2], \quad (59)$$

$$\frac{\partial N_d(\mathbf{q}_2)}{\partial t} = \lambda_m N_d(\mathbf{q}_2) + K N_d(\mathbf{q}_1) N_d(\mathbf{q}_3) - \gamma N_d(\mathbf{q}_2)[N_d(\mathbf{q}_1)^2 + N_d(\mathbf{q}_2)^2 + N_d(\mathbf{q}_3)^2], \quad (60)$$

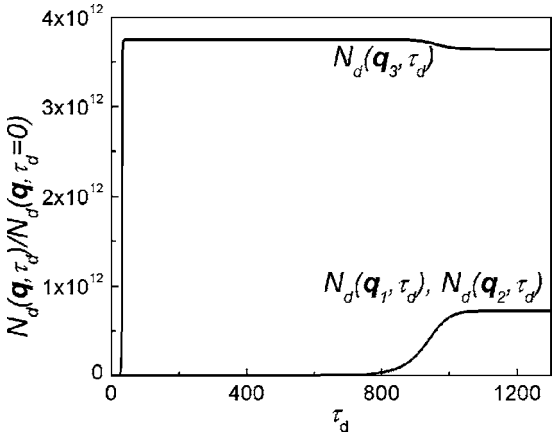

FIG. 5. The dependence of the Fourier amplitudes of the concentration of surface defects $N_d(\mathbf{q}_1, \tau_d)$, $N_d(\mathbf{q}_2, \tau_d)$, and $N_d(\mathbf{q}_3, \tau_d)$ on the dimensionless time $\tau_d = \lambda_m t$, constructed according to the numerical solution of the system of equations (59)–(61) using the values of parameters: $\gamma/\lambda_m = 8/(N_{d0}N_{dc2}) = 10^{-26}$ cm^4, $K/\lambda_m = 3/N_{d0} = 4\times 10^{-14}$ cm^2, $1/(\tau\lambda_m) = 0.7$, and $\varepsilon = 1.6$.

$$\frac{\partial N_d(\mathbf{q}_3)}{\partial t} = \left(\varepsilon\lambda_m + \frac{1-\varepsilon}{\tau}\right) N_d(\mathbf{q}_3) + \varepsilon K N_d(\mathbf{q}_1) N_d(\mathbf{q}_2) - \varepsilon\gamma N_d(\mathbf{q}_3)[N_d(\mathbf{q}_1)^2 + N_d(\mathbf{q}_2)^2 + N_d(\mathbf{q}_3)^2], \tag{61}$$

where λ_m is given by Eq. (27), $\gamma = 2D_{d0}|\theta_d\theta_a|\eta_d^2 q_m^2/(k_B T)^2 > 0$, $K = (3D_{d0}\theta_d/2k_B T)\eta_d q_m^2 > 0$, and $\varepsilon = D_{d0}/D_{d0} = 1 + |\theta_a \xi_e|/k_B T > 1$. In the system of equations (59)–(61) retained quadratic terms describe intermode interactions, while cubic terms besides intermode interactions describe also intramode nonlinearity. The numerical solution of the system (59)–(61) is shown in Fig. 5. Compressive stress is applied along the wave vector $\mathbf{q}_3$.

It is seen from Fig. 5 that the steady-state Fourier amplitude $N_d(\mathbf{q}_3)$ of $\mathbf{q}_3$ grating is roughly five times larger than Fourier amplitudes $N_d(\mathbf{q}_1)$ and $N_d(\mathbf{q}_2)$. The values of steady-state Fourier amplitudes $N_d(\mathbf{q}_1)$, $N_d(\mathbf{q}_2)$, and $N_d(\mathbf{q}_3)$ found analytically from the system (59)–(61) (by setting the left-hand sides of equations equal to zero) coincide with the corresponding values found by numerical integration of this system.

If, on the contrary, the tensile stress is applied along $\mathbf{q}_3$ ($\xi_e > 0$), then the $\mathbf{q}_3$ grating is suppressed. For comparison with experimental results see Sec. V.

V. COMPARISON WITH EXPERIMENTAL RESULTS: CONCLUSION

Recently, the formation of a virtually close-packed arrangement of Ga nanoparticles [Fig. 6(a)] with a narrow size distribution was observed in Ref. 3. The nanostructure was generated on the illuminated part of the tip of the silica optical fiber (in its core) upon the molecular-beam deposition of Ga atoms. The optical-fiber temperature was maintained at $T = 100$ K. Ga particles with a broad size distribution were formed in the part of the tip where laser radiation was absent.

The consideration made in Refs. 2 and 5, and in this work gives the following possible scenario of the formation of a nanoparticle ensemble with a narrow size distribution in the presence of laser radiation. A beam of Ga atoms is incident on the tip of an optical fiber with laser radiation introduced into it. Ga atoms are adsorbed on the tip surface and then become bound by a covalent bond in pairs, forming dimers analogous to the dimers in α-Ga crystal.[15] The absorption of radiation quantum ω with a wavelength of 1550 nm,[4] which lies inside the molecular absorption band of Ga dimers,[15] transfers the dimer from the ground state to an excited state. Relaxation from the excited state to the ground one proceeds through radiationless transitions with the liberation of energy $\leqslant\omega$. This energy decreases the activation energy of the surface diffusion of a dimer: $E_d \to E_d - \omega$, where E_d is the equilibrium activation energy of diffusion [see Eq. (5)]. In this case, the diffusion coefficient $D_d = D_0 \exp[-(E_d - \omega)/k_B T]$ increases, so that the diffusion of dimers in the illuminated area of the optical fiber tip occurs even at low temperatures. At the same time, the activation energy in the unilluminated area of the optical-fiber tip (outside its core) remains large, the diffusion coefficient remains relatively small, and the diffusion of dimers does not occur.

The mobile dimers can be considered as mobile defects on the surface (surface elastic inclusions) that can participate in the DD instability. Depending on the stage at which the cooperative nucleation process is terminated three types of DD structures can be formed: a random, quasihexagonal, or hexagonal one. In all these cases, the absolute strain extrema form a cellular structure on the surface and can serve as nucleation centers for the growth of the cellular nanostructure of Ga nanoparticles. In order to obtain a perfect hexagonal nanoparticle ensemble the deposition rate must be slow enough to ensure the completion of four stages of nonlinear evolution of DD seeding structure before the growing nanoparticles become immobile.

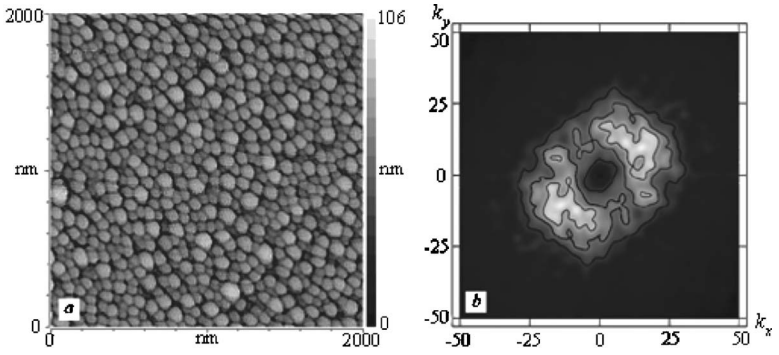

FIG. 6. (a) Atomic force microscopy (AFM) image of the illuminated area of the optical fiber tip after the deposition of Ga atoms during 30 min (by the results of Ref. 3); and (b) smoothed amplitude part $|F(k_x, k_y)|$ of the Fourier spectrum of the AFM image shown in (a); k_x and k_y are dimensionless wave numbers. The actual wave numbers are $q_x = 2\pi k_x/L_x$, $q_y = 2\pi k_y/L_y$, where $L_x = 2000$ nm, $L_y = 2000$ nm are the actual dimensions of the scanned surface area. Brighter areas correspond to larger values of $|F(k_x, k_y)|$.

The periodic surface strain field arising on the formation of the DD grating generates fluxes of mobile Ga clusters nucleated in a random way. These fluxes are directed toward the extrema of the strain. By virtue of this fact, only those clusters grow that reside at the extrema of the surface deformation field. Thus, after a certain time of growth, a close-packed arrangement of nanoparticles with a narrow size distribution forms in the illuminated surface area. This distribution is centered at a value proportional to the period Λ_m of the DD nanostructure (26). As follows from the results obtained in this work, the nucleation of the DD nanostructure can take place only at $T<T_c$ (29). This condition agrees with the results obtained in Ref. 3, where the nanostructuring of Ga was observed at $T=100$ K and was absent at $T=300$ K. In the area where there is no light, the Ga dimers are of low mobility at low temperatures, and the DD instability cannot occur. In this area, clusters nucleate in an individual, random way, and their growth also proceeds randomly. As a result, in the unilluminated area particles with a broad size distribution are formed.

In order to verify the prediction of possible hexagonal order in the arrangement of nanoparticles, a computer two-dimensional Fourier transformation of an AFM image of the surface after deposition [Fig. 6(a)] has been carried out in Ref. 5. A smoothed amplitude part of the Fourier spectrum $|F(k_x,k_y)|$ is shown in Fig. 6(b). The spectrum consists of the ellipsoidal ring of finite thickness, which corresponds to the random structure; but the traces of the angular self-organization—the occurrence of three pairs of intense maxima—are also clearly seen. Each pair, lying symmetrically with respect to the center of the ellipsoid on lines passing through its center, corresponds to the dominant grating of the local surface brightness of the image, that is, to the dominant grating of surface relief. Thus the pattern observed in Fig. 6(b) is formed by three groups of dominant surface relief gratings. Their wave vectors $\mathbf{q}$ are approximately equal to each other in magnitude and are directed at certain angles to each other, which corresponds to the occurrence of hidden long-range quasihexagonal order in the arrangement of nanoparticles.

The perfect hexagonal order in the case under consideration is disturbed for the following reasons. First, as is seen from Fig. 6(b) the collapse in scalar q-space did not occur at all or is uncompleted. Besides, the uniaxial strain of a certain sign (tensile or compressive) increases the diffusion coefficient along its direction (this strain can be caused by bending or twisting of the optical fiber). Therefore it "entraps" one of the DD gratings, orienting the grating vector along this direction, and makes this grating most intense (see Sec. IV D). This DD grating selected by the strain corresponds to the pair of the most intense maxima in Fig. 6(b). On the contrary, a strain of the opposite sign (compressive or tensile) leads to the repulsion of the DD grating vectors from their direction. As a result, three maxima on each side tend to group in the vicinity of the direction of enhanced diffusion. One may expect that the maxima will get closer with the increase of the strain until they merge completely into one maximum on each side of the diameter. The spectrum with two maxima, lying on the diameter of the circle, corresponds to one DD grating. Such a gradual transition from quasihexagonal to one-dimensional symmetry was realized recently in the experiment on etching of the ensemble of pores on nonuniformly strained Si plate.[16]

Let us perform some numerical estimations. At $|\theta_d|=10$ eV, $T=100$ K, $a=5\times10^{-8}$ cm, $\rho c_l^2=10^{12}$ erg cm^{-3}, and $\beta=0.3$ we estimate from Eq. (24) the first critical value of the uniform concentration of surface defects $N_{dc1}\approx2\times10^{12}$ cm^{-2}. At $|\theta_a|=1$ eV we estimate from Eq. (39) the second critical value $N_{dc2}\approx10^{13}$ cm^{-2}. Setting $\Lambda_m=d$ in Eq. (26), where $d\approx60$ nm is an experimentally observed nanoparticle size, we obtain the estimate for the scaling parameter $l_d\approx10$ nm. It can be shown that this value can be obtained in the model of surface dipoles (Ga dimers) interacting through long-range dipole field.

We note in conclusion that the theory presented in this paper is an approximate, mean-field-like theory. It could be validated by numerical solution of the full system of equations (18). It is obviously an interesting and necessary task, but it goes far beyond the scope of this paper. At the current stage the justification of the approximations made and the validation of the results obtained are based on their agreement with the experimental results. Besides, theoretical predictions made allow further experimental tests of this theory. In particular, the dynamics of self-organization of a hexagonal ensemble of adatom nanoparticles considered in this work can be studied experimentally by terminating the process of deposition at different time moments and performing Fourier transformation of the corresponding AFM images of the surface. In this way, for example, the four stage dynamics of formation of a perfect hexagonal ensemble of pores in oxidation of Al was revealed.[17]

ACKNOWLEDGMENT

This work has been carried out with partial support of the Engineering and Physics Science Research Council (EPSRC, United Kingdom), Project No. RG/R4441538/01.

*Corresponding author. Email address: emel@em.msk.ru

[1] V. Schukin and D. Bimberg, Rev. Mod. Phys. **71**, 1125 (1999).
[2] V. I. Emel'yanov and K. I. Eriomin, JETP Lett. **75**, 98 (2002).
[3] R. Brout, *Phase Transitions* (Benjamin, New York, 1965).
[4] K. F. MacDonald, V. A. Fedotov, S. Pochon, K. J. Ross, G. C. Stevens, W. S. Brocklesby, N. I. Zheludev, and V. I. Emel'yanov, Appl. Phys. Lett. **80**, 1643 (2002).
[5] V. I. Emel'yanov, K. I. Eriomin, and N. I. Zheludev, JETP Lett. **76**, 112 (2002).
[6] R. J. Asaro and W. A. Tiller, Metall. Trans. **3**, 1789 (1972).
[7] M. A. Grinfeld, Sov. Phys. Dokl. **31**, 831 (1986).
[8] D. J. Srolovitz, Acta Metall. **37**, 621 (1988).

[9] W. H. Yang and D. J. Srolovitz, Phys. Rev. Lett. **71**, 1593 (1993).
[10] I. A. Kunin, *Theory of Elastic Media with Microstructure* (Springer, Berlin, 1982).
[11] R. C. Picu, J. Mech. Phys. Solids **50**, 1923 (2002).
[12] M. J. Aziz, Defect Diffus. Forum **153**, 1 (1998).
[13] L. D. Landau and E. M. Lifshitz, *Theory of Elasticity* (Pergamon, New York, 1986).
[14] I. A. Viktorov, *Rayleigh and Lamb Waves* (Plenum Press, New York, 1970).
[15] X. G. Gong, G. L. Chiarotti, M. Parrinello, and E. Tosatti, Phys. Rev. B **43**, 14277 (1991).
[16] V. I. Emel'yanov, K. I. Eriomin, V. V. Starkov, and E. Yu. Gavrilin, Tech. Phys. Lett. **29**, 226 (2003).
[17] V. I. Emel'yanov, V. V. Igumnov, and V. V. Starkov, Tech. Phys. Lett. **30**, 438 (2004).